Organelle–nucleus cross-talk regulates plant intercellular communication via plasmodesmata

Tessa M. Burch-Smith[a], Jacob O. Brunkard[a], Yoon Gi Choi[b], and Patricia C. Zambryski[a,1]

[a]Department of Plant and Microbial Biology and [b]Functional Genomics Laboratory, University of California, Berkeley, CA 94720

Contributed by Patricia C. Zambryski, October 19, 2011 (sent for review June 20, 2011)

We use *Arabidopsis thaliana* embryogenesis as a model system for studying intercellular transport via plasmodesmata (PD). A forward genetic screen for altered PD transport identified *increased size exclusion limit* (*ise*) *1* and *ise2* mutants with increased intercellular transport of fluorescent 10-kDa tracers. Both *ise1* and *ise2* exhibit increased formation of twinned and branched PD. *ISE1* encodes a mitochondrial DEAD-box RNA helicase, whereas *ISE2* encodes a DEVH-type RNA helicase. Here, we show that ISE2 foci are localized to the chloroplast stroma. Surprisingly, plastid development is defective in both *ise1* and *ise2* mutant embryos. In an effort to understand how RNA helicases that localize to different organelles have similar impacts on plastid and PD development/function, we performed whole-genome expression analyses. The most significantly affected class of transcripts in both mutants encode products that target to and enable plastid function. These results reinforce the importance of plastid-mitochondria-nucleus cross-talk, add PD as a critical player in the plant cell communication network, and thereby illuminate a previously undescribed signaling pathway dubbed organelle–nucleus-plasmodesmata signaling. Several genes with roles in cell wall synthesis and modification are also differentially expressed in both mutants, providing new targets for investigating PD development and function.

embryo lethal | tiling arrays | virus-induced gene silencing | intracellular signaling

Plant cells are bound by cellulosic cell walls, creating a challenge to resource sharing and information exchange among individual cells. Overcoming this, plants have evolved channels that connect each cell to its immediate neighbors. Each channel, or plasmodesma, is delimited by the plasma membranes of the cells it connects and contains at its axial center strands of the endoplasmic reticulum (ER) that are continuous between cells. The space between the plasma and ER membranes is shared cytoplasm. Thus, plasmodesmata (PD) are cytoplasmic membrane-lined channels that facilitate the transport of biological molecules across cells. PD that form at cell division, when ER strands are trapped in the nascent cell wall, are called primary PD. Secondary PD arise independent of cytokinesis by a process that is not well understood but involves extensive remodeling of the cell wall and the endomembrane system (1). Both primary and secondary PD can be either simple linear channels or more elaborate and branched.

Small molecules like water, ions, and solutes move between cells via PD by diffusion along a concentration gradient (reviewed in 2). PD also have essential roles in the transport of larger molecules, including RNA, proteins, and viruses that impinge on the critical processes of development and growth. PD themselves are regulated by developmental and physiological signals from the plant (reviewed in 3). One approach to understanding the function and development of PD has been to identify the protein constituents of PD. For example, proteomic approaches (reviewed in 4) identified members of a class of callose-binding proteins that localize to PD, including PD-callose–binding protein1 (PDCB1) (5), and a β-1,3-glucanase enzyme that degrades the polysaccharide callose (β-1,3-glucan) (6). These proteins regulate PD aperture and transport by either depositing or removing callose from the cell walls surrounding PD openings. PD also contain cytoskeleton-associated proteins, including actin (7) and myosin (8). Proteins with potential roles in signal transduction are also PD constituents, such as a calcium kinase (9), calreticulin (10), a kinase that phosphorylates viral movement proteins (11), and membrane receptor-like proteins [PD-localized proteins (PDLPs)] (12). Remorin, a lipid-raft protein, was also recently found to localize to PD (13). Several additional potential membrane-bound PD-localized proteins have recently been reported (14).

We conducted a genetic screen of embryo-lethal mutants to identify genes critical to regulating PD function (15). We have mapped and cloned two genes, *INCREASED SIZE EXCLUSION LIMIT (ISE)1* and *ISE2*, that, when mutated, result in increased intercellular transport of fluorescent 10-kDa dextrans at the midtorpedo stage of embryogenesis. In addition to increased PD trafficking, *ise1* and *ise2* mutants display increased proportions of twinned and branched PD compared with WT embryos (16–18); this increase is likely attributable to more de novo production of secondary PD. In support, reduction of *ISE1* and/or *ISE2* transcript levels in mature leaves by gene silencing causes specific increases in secondary PD concomitant with increased PD transport (18).

ISE1 encodes a predicted DEAD-box RNA helicase that localizes to mitochondria (17). *ISE2* encodes a predicted DEVH-type RNA helicase (16), and microscopic examination of transgenic plants constitutively expressing ISE2 tagged at its C terminus with GFP (ISE2-GFP) suggested that ISE2-GFP localized to granules that were often associated with chloroplasts (figure 8A of ref. 16) or, less frequently, with a marker for plant RNA processing bodies, mRNA decapping enzyme 2 (DCP2)-RFP (figure 9 of ref. 16). Other data, however, suggested an alternative subcellular localization for ISE2:

i) The subcellular localization program TargetP (19) predicts that ISE2 possesses an N-terminal cleavable chloroplast transit peptide.

ii) A fusion of GFP to the first 100 N-terminal amino acids of ISE2 that contains the predicted chloroplast transit peptide localizes to chloroplasts (20).

iii) Proteomic analyses consistently identified ISE2 in chloroplast extracts (21, 22). Further, ISE2 fractionates with high-molecular-weight complexes (1–3 MDa) of the chloroplast stroma (22), consistent with our observation of its localization to relatively large foci.

Author contributions: T.M.B.-S., J.O.B., and P.C.Z. designed research; T.M.B.-S. and J.O.B. performed research; Y.G.C. contributed new reagents/analytic tools; T.M.B.-S. and J.O.B. analyzed data; and T.M.B.-S., J.O.B., and P.C.Z. wrote the paper.

The authors declare no conflict of interest.

Data deposition: The data reported in this paper have been deposited in the Gene Expression Omnibus (GEO) database, www.ncbi.nlm.nih.gov/geo (accession no. GSE33558).

[1]To whom correspondence should be addressed. E-mail: zambrysk@berkeley.edu.

See Author Summary on page 20297.

This article contains supporting information online at www.pnas.org/lookup/suppl/doi:10.1073/pnas.1117226108/-/DCSupplemental.

iv) In our gene silencing studies, we observed that loss of ISE2 resulted in severe leaf chlorosis (18).

We therefore performed more careful studies of ISE2-GFP localization, and our results reveal that ISE2 is a plastid protein.

The localization of ISE2 to plastids and the known localization of ISE1 to mitochondria (17) provoke a new question: How can two mutants encoding products that localize to different cellular compartments both exhibit the same strong effect on PD formation and function? The present analyses seek to provide the answer. We performed gene expression analyses comparing *ise1* and *ise2* mutants with WT embryos using whole-genome tiling microarrays to identify genes or processes that were similarly affected in both mutants. Notably several genes previously implicated in PD structure or function were differentially expressed in the mutants. Most importantly, the data reveal that both mutants have dramatic effects on genes involved in chloroplast function. Loss of ISE1 alters the abundance of nucleus-encoded mitochondria-related transcripts, as does loss of plastid ISE2, emphasizing plastid-mitochondria-nucleus cross-talk. Together, the data demonstrate that organelle–nucleus communication is essential for regulating all aspects of cellular physiology, including processes like cell wall formation and PD-mediated intercellular communication.

Results

ISE2 Is Found in Chloroplasts. To resolve ISE2's subcellular localization conclusively, we performed careful microscopic examination of ISE2-GFP in both transgenic and transient expression systems. Confocal microscopy of transgenic *Arabidopsis thaliana* or *Nicotiana benthamiana* plants expressing *ISE2-GFP*, and of *N. benthamiana* leaves transiently expressing *ISE2-GFP*, consistently revealed that ISE2-GFP formed foci that were always associated with chloroplasts (Fig. 1 *A*–*C*). Time-lapse confocal microscopy of *N. benthamiana* plants transiently expressing ISE2-GFP shows that the ISE2-GFP forms discrete foci that always associate with chloroplasts as the chloroplasts stream through the cell (Movie S1). The presence of ISE2 in chloroplasts helps explain why silencing of *ISE2* in *N. benthamiana* leaves by Tobacco rattle virus (TRV)-based gene silencing results in severe chlorosis (Fig. 1*E*).

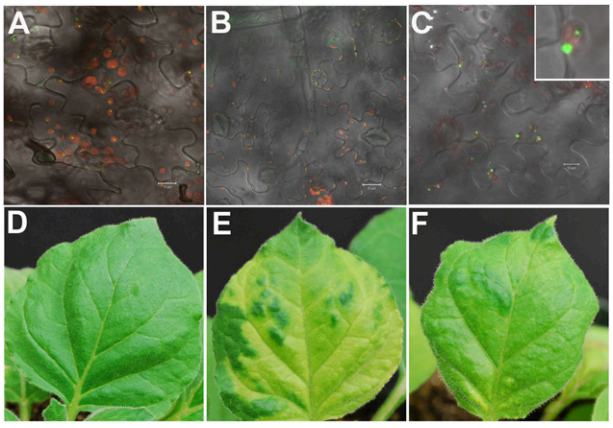

Fig. 1. ISE2 is chloroplast-localized, and loss of ISE1 or ISE2 causes chlorosis. ISE2-GFP localizes to foci in chloroplasts in transgenic *A. thaliana* (*A*) and transgenic *N. benthamiana* (*B*) and when transiently expressed in *N. benthamiana* (*C*). Magnified view of a chloroplast in *Inset*. Red signal is chlorophyll autofluorescence. (Scale bars: *A* and *C*, 10 μm; *B*, 20 μm.) (*D*–*F*) Upper leaves of silenced *N. benthamiana* plants 14 d after infiltration of TRV-virus-induced gene silencing vectors. (*D*) Leaves in nonsilenced TRV-infected control *N. benthamiana* plants are uniformly green. (*E*) Severe chlorosis in *ISE2*-silenced leaves. (*F*) Moderate chlorosis in *ISE1*-silenced leaves.

We next examined the ultrastructure of plastids in *ise* mutants compared with WT embryos. Embryo "greening" usually occurs between the late heart and early torpedo stages of embryogenesis, about 96 h after fertilization, marking the switch from heterotrophic to autotrophic growth. At this time, plastids contain rudimentary grana and begin the "maturation phase" of embryogenesis with the synthesis of oil and protein stores (23). The plastids of midtorpedo stage *ise2 A. thaliana* embryos contain fewer thylakoid membranes arranged in grana compared with WT embryos (Fig. 2 *A* and *B*). To investigate further the role of ISE2 in plastid development, we examined leaves in *N. benthamiana* plants following TRV-induced gene silencing of *ISE2*. Chloroplasts in nonsilenced TRV-infected leaves contained typical stacked thylakoids as expected (Fig. 2*D*). In *ISE2*-silenced leaves, however, chloroplasts contained fewer thylakoids and an increase in stromal volume (Fig. 2*E*). Aberrant plastids containing plastoglobules were found in transgenic plants overexpressing *ISE2* (20). Thus, *ISE2* has a critical role in plastid development and function.

Unexpectedly, plastids in *ise1* embryos and chloroplasts in *ISE1*-silenced leaves also show aberrant development (Fig. 2 *C* and *F*), although there is less chlorosis in *ISE1*-silenced leaves (Fig. 1*F*). Loss of mitochondrial function therefore has a major impact on plastid function and development, a result supported by our gene expression analyses described below.

Gene Expression Analyses in *ise1* and *ise2* Embryos. To understand how mutation of either a mitochondrial (ISE1) or plastid (ISE2) RNA helicase results in the similar phenotypes of increased PD transport and defective plastids, we examined changes in gene expression in *ise1* and *ise2*. By sampling a single stage in development, the data reveal a snapshot of the steady-state RNA levels in the mutants compared with WT embryos. The RNA levels reflect transcription as well as RNA processing and stability. For example, there is limited transcriptional regulation of gene expression in mitochondrial and plastid genomes (24). It is also well known that differences in RNA levels do not necessarily reflect changes in protein content. Nevertheless, for clarity, we refer here to all changes in transcript levels as changes in expression levels and assume that these changes generally lead to altered protein production.

The *ise1* and *ise2* mutants were originally identified on the basis of their continued ability to transport large (10 kDa) fluorescent dextrans in the midtorpedo stage of embryogenesis, a time when intercellular transport is significantly down-regulated in WT embryos (15). We therefore chose to examine embryo transcripts at this stage of development. The *ise1-2* and *ise1-3* null mutants arrest development before reaching the midtorpedo stage; thus, we used the point mutant *ise1-1* that develops to the torpedo stage (17) for our analysis. All *ise2* mutants arrest at the midtorpedo stage of development (16) when photosynthesis normally initiates; for our analyses, we used the *ise2-1* point mutant. Seeds from *ise1-1* or *ise2-1* heterozygotes were planted, and the siliques of the resulting self-fertilized plants were screened to identify homozygous-mutant embryos. Developing seeds containing midtorpedo stage homozygous mutant embryos are albino and easily distinguished from their green WT siblings.

Fig. S1 describes the workflow for preparing samples from seeds collected for gene expression analyses. Plastids and mitochondria have important roles in sensing and responding to environmental stresses (25), and PD are rapidly altered in response to wounding and mechanical stress (26). We wanted to avoid inducing stress responses in the tissue under investigation, and therefore collected developing whole seeds containing midtorpedo stage embryos. Thus, the RNA extracted represents transcripts from genes expressed in developing endosperms, seed coats, and midtorpedo stage embryos. Biotin-labeled cDNA was used to interrogate the Affymetrix GeneChip *Arabidopsis* 1.0R

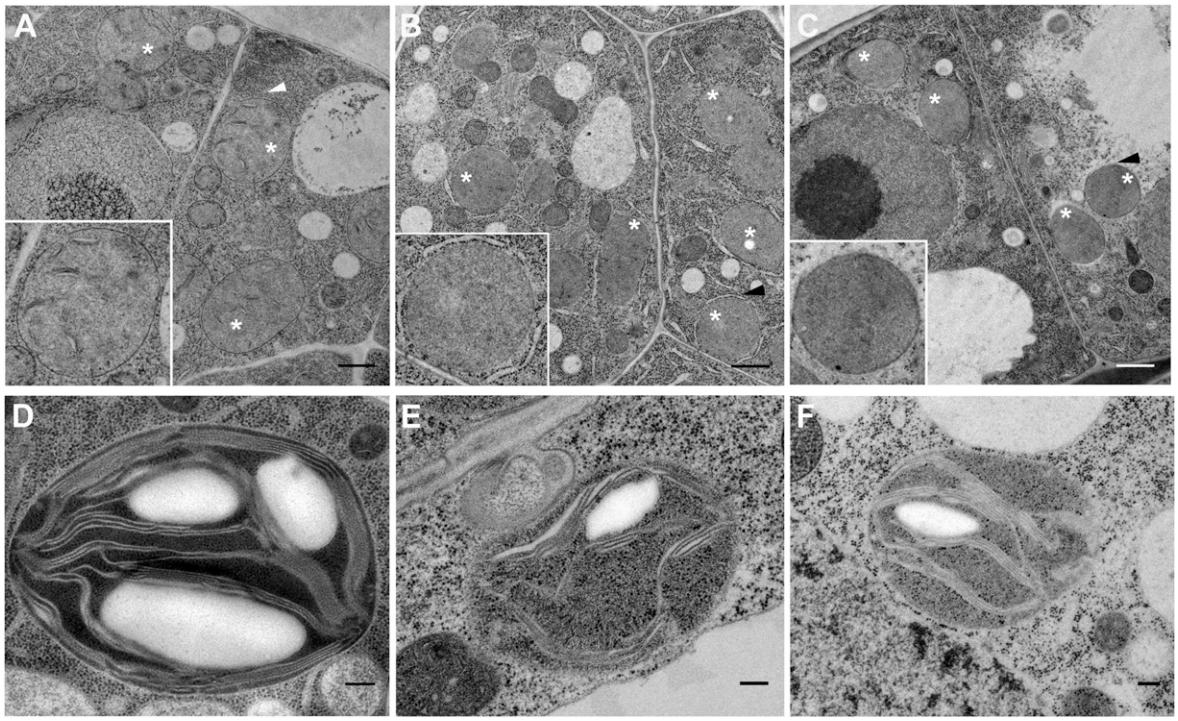

Fig. 2. Loss of ISE2 or ISE1 alters plastid development. (*A*–*C*) Plastids in *A. thaliana* embryos. (*A*) Plastids in WT midtorpedo stage *A. thaliana* embryos contain thylakoids arranged into rudimentary grana. Plastids in *ise2* (*B*) or *ise1* (*C*) midtorpedo stage embryos contain no grana. Plastids are marked with white asterisks. (*Insets*) Plastids highlighted by black or white arrowheads are shown. (Scale bars: 1 μm.) (*D*–*F*) Chloroplasts in silenced *N. benthamiana* leaves. (*D*) Chloroplasts in nonsilenced TRV-infected control leaves contain extensive grana and several large starch grains. (*E*) Chloroplasts in *ISE2*-silenced leaves contain fewer grana, fewer starch grains, and greater stromal fraction than in nonsilenced control leaves. (*F*) Chloroplasts in *ISE1*-silenced leaves are intermediate between those in nonsilenced controls and in *ISE2*-silenced plants, with reduced grana and starch granule formation and increased stromal fraction. (Scale bars: 200 nm.)

Tiling Array. We chose to perform microarray-based analyses rather than direct RNA sequencing because of the current abundance of statistical and other tools for array data analyses. We used the tiling array instead of the more commonly used Affymetrix ATH1 array because 30,228 genes are represented on the tiling array compared with only 20,719 on the ATH1 array (27). Many of the 9,645 genes found exclusively on the tiling array are normally expressed at very low levels. Several studies have shown the GeneChip *Arabidopsis* 1.0R Tiling Array to be a robust platform for studying changes in expression of genes not easily detected by or absent from the ATH1 array (28, 29).

General Patterns of Gene Expression. Embryos express a large fraction of the genome. Studies using the ATH1 arrays estimate that between 51% and 77% of genes are expressed in torpedo stage embryos (30). For our analyses, we selected genes exhibiting twofold or greater changes in expression compared with WT embryos. This produced a list of 2,943 genes with altered expression in *ise1* and 3,704 genes with altered expression in *ise2* (Fig. 3*A*). A total of 1,333 genes were commonly affected in both mutants (Fig. 3*B*). A complete list of all the genes affected is found in Dataset S1.

Genes whose products are directly involved in plastid function are profoundly affected in both mutants. Of the 1,333 genes commonly affected in *ise1* and *ise2*, 943 have assigned functions; of those, 18% encode plastid-related products (Dataset S1). Fig. 3*C* displays the changes (increased or decreased) in gene expression in each mutant individually, with 348 genes related to plastid processes exhibiting altered expression in *ise1* and 375 in *ise2* (Fig. 3*C*). Gene expression related to mitochondrial processes also was affected in *ise1* or *ise2*, although, surprisingly, more mitochondrial genes showed altered expression in *ise2* (156 genes) than in *ise1* (114 genes) (Fig. 3*C*). Genes encoding products with roles in nuclear transcription were affected in each mutant: 158 in *ise1* compared with 192 in *ise2*. Because *ise1* and *ise2* mutants both show altered PD formation, we were particularly interested in any changes in expression of genes related to cell wall synthesis and modification. Similar numbers of genes (~100) showed altered expression in each mutant (Fig. 3*C*). Although both *ise1-1* and *ise2-1* mutants show retarded development, the expression of relatively few genes involved in control of growth and development was affected in *ise1* (52 genes) and *ise2* (61 genes). We used quantitative real-time PCR for a set of 19 genes in different cellular processes and confirmed the changes in transcript levels detected by the microarray analyses. We next describe the changes in expression observed for four classes of genes most relevant to the phenotype of *ise1* and *ise2*: nuclear-encoded plastid genes, genes for cell wall and PD localized products, nuclear-encoded mitochondrial genes, and organelle (plastid and mitochondria) genes.

Plastid-Related Gene Expression in *ise1* and *ise2* Embryos. Because torpedo stage embryos should be initiating photosynthesis, we determined which of the affected genes (Fig. 3 and Table S1) encode products with roles in chlorophyll biosynthesis, the light reactions of photosynthesis, and the Calvin–Benson cycle (Fig. 4). Strikingly, the affected genes are almost uniformly down-regulated, exemplified by 89% (63 of 71) of the genes shown in Fig. 4 and Table S1. Indeed, 93% (39 of 42) of the nucleus-encoded genes whose products participate in the light-dependent reactions of photosynthesis are down-regulated in the two mutants (Fig. 4*C*), suggesting that photosynthesis is severely inhibited.

The repression of genes involved in chlorophyll biosynthesis (Fig. 4*B*), in addition to the decreased expression of genes for

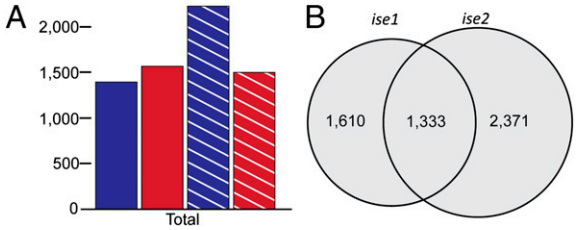

	Plastid	Mitochondria	Nuclear Transcription	Cell Wall	Cell Growth and Division
ise1 up	102	54	68	43	21
ise1 down	246	60	90	55	31
ise2 up	158	109	100	63	33
ise2 down	217	47	92	46	28

Fig. 3. Genes with changes in expression in *ise1* or *ise2* midtorpedo stage mutants compared with WT tissues. (*A*) Approximately the same number of genes (~1,500) show increased or decreased expression in *ise1*. More genes are induced vs. repressed in *ise2*. The data were complied from genes showing twofold or greater changes in expression compared with WT samples, with $P < 0.05$. (*B*) Large numbers of genes have altered expression in both mutants. (*C*) Number of genes encoding products with functions in selected processes exhibiting altered expression in *ise1* or *ise2*. The largest group of genes affected in both *ise1* and *ise2* encode products that affect plastid function. Gene functions were assigned as described in *Materials and Methods*.

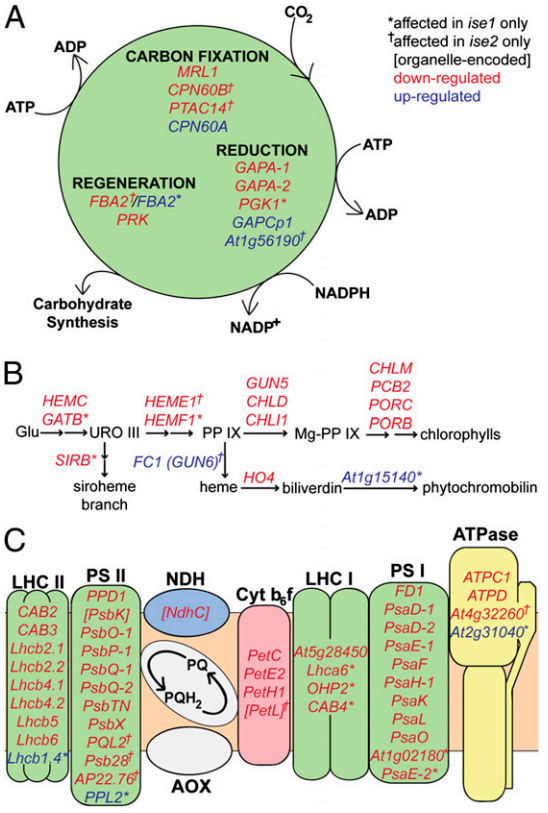

Fig. 4. Genes encoding plastid proteins exhibit altered expression in *ise1* or *ise2*. (*A*) Genes for Calvin–Benson cycle components with altered expression levels in *ise1* or *ise2* compared with WT. (*B*) Genes for tetrapyrrole synthesis with altered expression levels in *ise1* or *ise2* compared with WT. (*C*) Genes for photosynthetic electric transport chain components with altered expression in *ise1* or *ise2* compared with WT. Most affected genes are repressed in mutants compared with WT. Genes in brackets are encoded by the plastid genome; all other genes are nuclear. Because of space considerations, gene names are abbreviated. Their full names are given in Table S1.

light harvesting complexes and photosystems (Fig. 4*C*), explains the white color of the mutant embryos. Genes for the Calvin–Benson cycle are also largely down-regulated, indicating that carbon fixation is limited in the mutants (Fig. 4*A*). Importantly, the data dramatically reveal that loss of mitochondrial function in *ise1* also leads to repression of nuclear expression of genes with functions in the plastids. These results highlight the importance of intracellular communication among organelles during development. The data further suggest that loss of mitochondrial and/or chloroplast function signals to the nucleus to inhibit further expression of nucleus-encoded plastid genes.

The observed down-regulation of plastid-specific gene products in the mutant embryos is consistent with the fact that nuclear genes encoding photosynthesis-related proteins normally are up-regulated in WT torpedo *A. thaliana* embryos compared with the late heart and globular stages (30).

Loss of *ISE1* or *ISE2* Alters Expression of PD and Cell Wall Genes. In addition to the dramatic down-regulation of nucleus-encoded plastid-related genes, whole-genome expression analyses of *ise1* and *ise2* reveal changes in expression of genes that might be expected to alter PD formation/function directly. Several genes previously reported to localize to PD or regulate PD function are differentially regulated in *ise1* or *ise2* mutant embryos (Table 1). Callose is a crucial player in regulating PD aperture and transport (26). Genes regulating callose synthesis (e.g., *CHORUS/GLUCAN SYNTHASE-LIKE 8*) or callose degradation [e.g., *ATBETA-1,3-GLUCANASE_PUTATIVE PLASMODESMATAL ASSOCIATED PROTEIN* (*ATBG_PPAP*)] are well represented in our dataset. Unexpectedly, genes predicted to decrease PD size exclusion limits, including *REVERSIBLY GLYCOSYLATED POLYPEPTIDE* (*RGP3*) (31) and *PDLP5*, *PDLP6*, and *PDLP8* (12), exhibit increased expression in *ise1* and *ise2* mutants (Table 1). Similarly, expression of *ATBG_PPAP* is expected to increase PD size exclusion limits through callose removal (6), but *ATBG_PPAP* expression is down-regulated in *ise1* and *ise2* mutants (Table 1).

Numerous genes with functions in cell wall biogenesis and modification are differentially regulated in *ise1* or *ise2* tissues (Table 2 and Dataset S1). Many of these likely are involved in the generation of cell wall precursor units (Dataset S1). Cellulose synthases (CESAs) and cellulose synthase-like proteins (CSLs) are a superfamily of glycosyltransferases involved in the synthesis of cell wall polysaccharides (32). The *A. thaliana* genome encodes 10 *CESA* genes and 29 *CSL* genes, divided into six groups. The *CESA* genes have roles in cellulose synthesis: *CESA1*, *CESA3*, and *CESA6* are essential for general cellulose synthesis, and *CESA4*, *CESA7*, and *CESA8* are important for cellulose synthesis in secondary cell walls (33). The *ise1* and *ise2* mutants exhibit several fold changes in expression of *CESA1*, *CESA2*, *CESA3*, and *CESA8* (Table 2).

In *A. thaliana*, CSLs are involved in the synthesis of the hemicelluloses xyloglucan (XyG) (specifically, the subfamily CSLCs) and glucomannan (CSLAs and CSLDs) (32). XyGs are found in the cell walls of land plants and may comprise up to 20% of the dry weight of the walls in dicots (34). XyGs play a critical structural role in the cell wall by cross-linking with cellulose fibrils. Four *CSLC* genes, *CSLC4*, *CSLC5*, *CSLC6*, and *CSLC12*, are differentially expressed in *ise1* and *ise2* compared with WT tissues (Table 2). Notably, in *ise1* mutants, *CSLC5* is 15-fold repressed

Table 1. Changes in PD-related gene expression in *ise1* and *ise2* mutants compared with WT

Locus	Gene name	Fold change in expression	
		ise1	*ise2*
At5g42100	*AT-β-1,3-GLUCANASE_PUTATIVE PLASMODESMATAL ASSOCIATED PROTEIN*	−2.7	−3.8
At4g26100	*CASEIN KINASE 1*		+4.0
At2g36850	*CHORUS (GLUCAN SYNTHASE-LIKE 8)*	+3.3	−4.3
At1g70070	*INCREASED SIZE EXCLUSION LIMIT 2*	−3.9	
At1g18650	*PD CALLOSE BINDING PROTEIN 3*	−3.3	−3.3
At1g70690	*PD LOCALIZED PROTEIN 5*		+5.5
At2g01660	*PD LOCALIZED PROTEIN 6*		+2.2
At3g60720	*PD LOCALIZED PROTEIN 8*	+3.2	
At3g08900	*REVERSIBLY GLYCOSYLATED PROTEIN* 3		+2.9

compared with WT. Three *CSLD* genes *(CSLD2*, *CSLD3*, and *CSLD5*) and one *CSLA* gene (*CSLA9*) also show altered expression in *ise1* and *ise2* mutants (Table 2).

A large family of 33 XyG endotransglucosylase/hydrolase (XTH) enzymes is involved in XyG modification in *A. thaliana*, and the expression of *XTH* genes is tissue-specific (35). Eight of these genes are differentially regulated in *ise1* and/or *ise2* compared with WT (Table 2). *XTH19* has been reported as root-specific (36, 37), yet it is strongly induced in both mutants. Indeed, *XTH19* is the most strongly induced gene in *ise1* (50-fold higher than WT levels), and it is also strongly induced in *ise2* (15-fold WT levels). Other *XTH* genes that are differentially regulated in *ise1* and *ise2* show smaller changes in expression (2.1- to 6.9-fold) compared with WT tissues (Table 2).

Expansins are a superfamily of proteins that mediate acid-induced cell wall expansion by the process of molecular creep (38). There are four families of expansins, two of which, α-expansins (EXPAs) and β-expansins (EXPBs), are involved in cell wall loosening, mediating cell growth and development. The *A. thaliana* genome contains 26 EXPA and 6 EXPB genes, in addition to 3 expansin-like A and 1 expansin-like B genes (38). Nine of these 36 expansins are differentially expressed in the *ise* mutants (Table 2). With the exception of induced expression of α-*EXPANSIN 20* (*EXPA20*) in *ise2* seeds, all are moderately repressed in *ise1* and *ise2* mutants.

Genes Affecting Mitochondrial Function. Numerous nuclear genes encoding products with mitochondrial functions are differentially affected in *ise1* and *ise2* mutants (Dataset S1). The major function of mitochondria in embryos is carbohydrate metabolism for ATP production; we therefore examined the expression of genes specifically related to these processes (Fig. 5 and Table S2). Indeed, many affected genes encode proteins involved in the transport of metabolites into and out of the mitochondria (Fig. 5*A*), the mitochondrial electron transport chain (mETC) (Fig. 5*B*), and the tricarboxylic acid cycle (Fig. 5*C*). Unlike the pattern observed for photosynthesis-related genes, however, different genes are affected in the two mutants and there is no clear bias toward repressing gene expression. The most likely effect of these changes on mitochondrial function is to reduce both flux through the mETC and ATP production. Decreased energy availability almost certainly contributes to the reduced growth rates and stunted development of the mutants.

It is no surprise that compromised mitochondrial function in *ise1* embryos signals the nucleus to regulate transcripts encoding mitochondrial products; however, compromised chloroplast function in *ise2* also affects transcripts encoding mitochondrial products. Of special note in *ise2* mutants is the induction of the *ALTERNATIVE OXIDASE 1a* (*AOX1a*) gene, a marker for mitochondria-to-nucleus retrograde signaling (39), and genes encoding several external alternative mitochondrial *NAD(P)H DEHYDROGENASE*s (*NDB2*, *NDB3*, and *NDB4*; Fig. 5). These NDBs oxidize intermembrane NADH to reduce ubiquinone (UQ) to UQH_2, which is, in turn, oxidized by AOX1a to reduce oxygen to water in the mitochondrial matrix. When induced, this process effectively bypasses mETC complexes I–IV, transferring electrons into the mitochondrial matrix without pumping protons to the intermembrane space. The coordinated expression of AOX1a and these NDBs thus constitutes a dissipating system

Table 2. Selected cell wall-related genes have altered expression in *ise1* and *ise2* mutants

Locus	Gene name	Fold change in expression	
		ise1	*ise2*
CESAs and CSLs			
At4g32410	*CELLULOSE SYNTHASE 1*		+3.8
At4g39350	*CELLULOSE SYNTHASE 2*		−2.5
At5g05170	*CELLULOSE SYNTHASE 3*	+3.2	
At4g18780	*CELLULOSE SYNTHASE 8*	+3.2	+2.2
At5g03760	*CELLULOSE SYNTHASE-LIKE A9*	−3.7	
At3g28180	*CELLULOSE SYNTHASE-LIKE C4*		+3.7
At4g31590	*CELLULOSE SYNTHASE-LIKE C5*	−15.3	
At3g07330	*CELLULOSE SYNTHASE-LIKE C6*	+2.8	
At4g07960	*CELLULOSE SYNTHASE-LIKE C12*	−6.4	−2.6
At5g16910	*CELLULOSE SYNTHASE-LIKE D2*	+2.3	+3.0
At3g03050	*CELLULOSE SYNTHASE-LIKE D3*		+2.1
At1g02730	*CELLULOSE SYNTHASE-LIKE D5*	+6.1	
Expansins			
At2g37640	α-*EXPANSIN 3*		−2.4
At2g39700	α-*EXPANSIN 4*	−2.5	
At3g29030	α-*EXPANSIN 5*	−3.0	−2.7
At3g03220	α-*EXPANSIN 13*	−6.0	
At2g03090	α-*EXPANSIN 15*	−2.4	−2.4
At4g38210	α-*EXPANSIN 20*		+2.7
At2g20750	β-*EXPANSIN 1*	−2.4	
At1g65680	β-*EXPANSIN 2*	−3.9	
At2g45110	β-*EXPANSIN 4*	−3.5	−2.9
XTHs			
At2g06850	*XTH4*	+4.9	+6.9
At5g13870	*XTH5*		+2.6
At5g57540	*XTH13*		+4.0
At4g30290	*XTH19*	+50.3	+15.0
At4g25810	*XTH23*	−4.5	−2.1
At4g30270	*XTH24*		+4.0
At1g14720	*XTH28*	+2.3	
At1g32170	*XTH30*	−3.5	+2.6

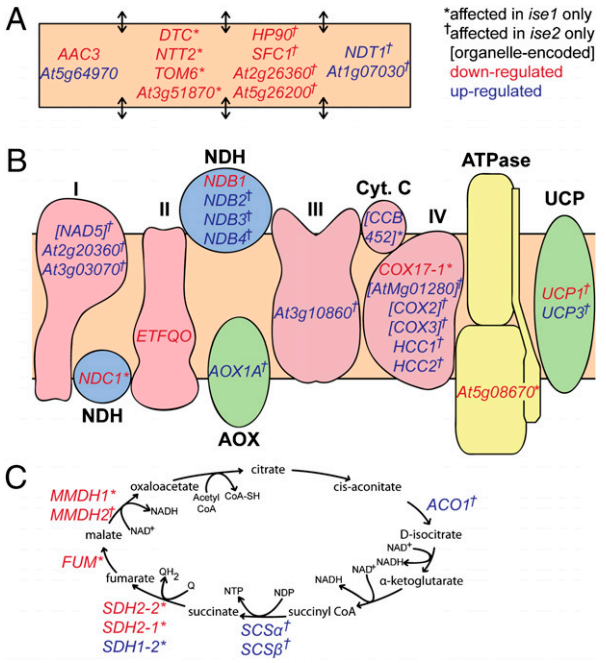

Fig. 5. Genes encoding mitochondrial proteins exhibit altered expression in *ise1* or *ise2*. (*A*) Genes encoding metabolite transporters are mostly repressed in *ise1* and *ise2* compared with WT. Different genes are affected in *ise1* and *ise2*. The peach color indicates the mitochondrial membrane, and the arrows indicate transport through the membrane into or out of mitochondria. (*B*) Genes encoding mETC components show altered expression in *ise1* or *ise2* compared with WT. Loss of ISE2 affects expression of more genes than does loss of ISE1. (*C*) Genes encoding enzymes of the tricarboxylic acid cycle. Five genes are affected in *ise1*, and three genes are affected in *ise2*. Genes in brackets are encoded by the mitochondrial genome; all other genes are nuclear. Because of space considerations, gene names are abbreviated. Their full names are given in Table S2.

Table 3. Mitochondrial gene expression is altered in *ise1* and *ise2*

Locus	Gene name	Fold change in expression	
		ise1	*ise2*
AtMg00180	*CYTOCHROME C BIOGENESIS 452*	+2.1	
AtMg00665	*NADH DEHYDROGENASE 5B*	+2.5	
AtMg01030	*ORF106E*	+2.0	
AtMg01060	*ORF107G*	+2.0	
AtMg00530	*ORF109*	+2.8	
AtMg01020	*ORF153B*	+3.4	
AtMg01050	*ORF159*	+2.4	
AtMg00610	*ORF161*	+4.3	
AtMg00880	*ORF187*	+6.7	
AtMg01110	*ORF251*	+2.7	
AtMg01090	*ORF262*	+5.0	
AtMg00670	*ORF275*	+2.4	+2.3
AtMg00160	*CYTOCHROME C OXIDASE SUBUNIT 2*		+2.0
AtMg00730	*CYTOCHROME C OXIDASE SUBUNIT 3*		+2.1
AtMg00770	*ORF100B*		+3.5
AtMg01180	*ORF111B*		−3.3
AtMg01290	*ORF111C*		+4.5
AtMg00150	*ORF116*		+3.1
AtMg00470	*ORF122A*		+2.3
AtMg01300	*ORF136A*		+3.1
AtMg01310	*ORF136B*		+3.1
AtMg00170	*ORF139A*		+2.2
AtMg01140	*ORF152B*		+2.2
AtMg00860	*ORF158*		+2.5
AtMg00140	*ORF167*		+2.7
AtMg01280	*ORF291*		+2.3
AtMg00590	*ORF313*		+2.6

for cellular NADH and typically decreases the production of reactive oxygen species (ROS) from the mETC. It is not clear, however, why both the mETC and the AOX/external NDBs would be induced in *ise2* mutants, given that there is likely to be a limited supply of NADH because of the lack of photosynthesis. Potentially, there are important differences in AOX function between embryos and mature plants. These findings illustrate the complexity of interorganelle communication in regulating cellular physiology.

Organelle-Encoded Transcripts Are Affected in *ise1* and *ise2*. The ISE1 and ISE2 RNA helicases likely are involved in processing transcripts of mitochondrial and plastid-encoded genes, respectively. Posttranscriptional modification and modulation of transcripts are major strategies for controlling expression of mitochondrial and plastid genes (24, 40). We therefore anticipated modest changes in the levels of organelle-encoded transcripts.

Mitochondrial genomes encode proteins that function in mitochondrial processes, particularly translation and oxidative phosphorylation (41). Examination of transcripts from *ise1* and *ise2* mutants revealed that numerous mitochondria-encoded genes are induced (Table 3); strikingly, different genes are affected in each mutant. Of the genes with known function, *nad5b* encoding a subunit of the NADH dehydrogenase of the respiratory chain complex I is up-regulated in *ise1*, and *cox2* and *cox3* encoding cytochrome *c* oxidase components are up-regulated in *ise2*. The *A. thaliana* mitochondrial genome also contains large numbers of ORFs of unknown function (42). ORF-encoding genes are the predominantly affected species in both *ise1* and *ise2*. Distinct ORFs are affected in each mutant with only *ORF275* commonly induced (~2.3-fold) in both *ise1* and *ise2* (Table 3). *ORF111B* is the only transcript that is down-regulated (in *ise2*). That mitochondrial transcripts also are affected in *ise2* is further evidence for signaling between mitochondria and plastids in the embryo.

The plastid genome encodes products with critical functions in photosynthesis, plastid gene expression, and fatty acid synthesis (43, 44). Table 4 reveals that several plastid transcripts are differentially down-regulated in both mutants. Unexpectedly, more transcripts were affected in *ise1* than in *ise2*. Several tRNA genes and a ribosomal gene are repressed in *ise1*, and a single ribosomal gene is induced, but none of these are affected in *ise2*. These data suggest that translation is inhibited in *ise1* plastids, leading to even more severe effects on plastid protein content than revealed by gene expression analyses. Indeed, plastids in *ise1* embryos, like those in *ise2* embryos, display severe defects in thylakoid stacking and lack rudimentary grana at the midtorpedo stage in contrast to their WT siblings (Fig. 2). These findings confirm that one of the major effects of the *ise1* mutation is to alter plastid function. Notably, *ycf1*, one of the three plastid-encoded genes described as absolutely essential for embryogenesis (43), is repressed in both *ise1* and *ise2* mutants (Table 4).

Discussion

The *A. thaliana ise1* and *ise2* mutations cause defective embryo development, increase cell-to-cell trafficking, and alter PD structure and formation (16–18). *ISE1* encodes a DEAD-box mitochondrial RNA helicase (17). *ISE2* encodes a DEVH RNA

Table 4. Plastid gene expression is altered in *ise1* and *ise2*

Locus	Gene name	Fold change in expression	
		ise1	*ise2*
AtCg00160	*RIBOSOMAL PROTEIN S2*	−4.9	
AtCg00770	*RIBOSOMAL PROTEIN S8*	+2.3	
AtCg00100	*tRNA-Gly-1*	−2.1	
AtCg00410	*tRNA-Phe*	−3.3	
AtCg00290	*tRNA-Ser-2*	−2.2	
AtCg00450	*tRNA-Valine 1*	−2.5	
AtCg00440	*NADH DEHYDROGENASE D3 SUBUNIT*	−2.4	−2.1
AtCg00070	*PS II REACTION CENTER PROTEIN K*	−2.5	−2.2
AtCg01130	*YCF1*	−2.6	−2.4
AtCg00590	*ORF31*		−2.3

helicase (16) that localizes to chloroplasts (Fig. 1 and Movie S1). Thus, disruption of two different organelle-specific RNA helicases produces similar phenotypes of altered PD structure/function and altered development. Whole-genome expression analyses of midtorpedo stage *ise1* and *ise2* embryos reveal that the most significant alterations are observed in nuclear genes encoding products with plastid functions. The remarkable number of nucleus-encoded, plastid-localized gene products that are commonly affected in *ise1* and *ise2* mutants illuminates our understanding of the numerous identical phenotypes of the mutants. In brief, the data support that plastids regulate embryo development, PD formation, and PD function. These and other alterations in gene expression are discussed below.

Altered PD Biogenesis in *ise1* and *ise2* Embryos. Genes with cell wall and PD-related functions are differentially expressed in mutant embryos compared with WT. Of particular interest is the large, 50- and 15-fold ectopic accumulation of *XTH19* transcripts in *ise1* and *ise2* mutants, respectively. XTH enzymes modify XyG during cell wall expansion. As secondary PD form in existing cell walls (18), there undoubtedly must be remodeling of the cell wall to permit the insertion of ER and plasma membranes to form PD (reviewed in 1). Thinning of cell walls occurs in tissues with extensive formation of secondary PD (45, 46). Perhaps XTH19 modifies XyG-cellulose associations to alter the cell wall at sites of de novo PD synthesis. We had anticipated that expansins might be up-regulated to loosen the cell wall for insertion of secondary PD, but most expansin genes exhibited reduced expression in our mutants, with only *EXPA20* showing increased expression in *ise2*. This suggests that XTHs, rather than expansins, are key regulators of cell wall modifications crucial for the insertion of secondary PD, at least during embryogenesis. Because secondary PD formation is dramatically increased in chlorotic *ISE2*-silenced leaves (18), it will be interesting to compare the expression of XTHs vs. expansins in this tissue.

Importantly, genes encoding known PD constituents or influencing PD structure exhibit altered expression in our mutants (Table 1). For example, genes for callose synthesis (*GSL8*, *RGP3*, and *PDCB3*) or removal (*ATBG_PPAP*) at PD neck regions are differentially expressed in *ise1* and *ise2* compared with WT embryos. A likely combined effect of alteration of genes encoding PD-localized and/or callose-regulating products is to alter PD transport, consistent with the phenotypes of *ise1* and *ise2* mutants. However, the direction of expression changes (increased or decreased) in these genes was the reverse of what one would predict if callose were involved in the changes in PD function we observe in the mutants. The data suggest that embryos may regulate PD differently than more mature tissues or that callose does not mediate the PD changes in *ise1* and *ise2* mutants.

Plastids and Mitochondria Are Essential for Embryogenesis. The identification and characterization of genes with critical functions during embryogenesis have been the focus of intense study (47, 48). A collection of embryo-defective mutants and their affected genes is curated at the SeedGenes database (48). Recent examinations of mutations that lead to defective embryogenesis (*emb* genes) reveal astonishing results: More than 30% of *emb* genes encode plastid-localized products (43, 50). This overrepresentation of genes encoding plastid proteins highlights the critical role of plastids in embryogenesis. According to Bryant et al. (43), the functions affected can be grouped into three categories: (*i*) enzymes involved in synthesis of fatty acids, vitamins, and other metabolites; (*ii*) proteins required for import, modification, and localization of plastid proteins; and (*iii*) proteins required for plastid translation.

Remarkably, mutants in individual genes encoding proteins directly involved in photosynthesis are not lethal (43). RNA helicases are RNA-binding proteins involved in all aspects of RNA metabolism, including transcription, splicing, ribosome biogenesis, nuclear export, and translation (reviewed in 51, 52). Thus, loss of such function in *ise2* likely leads to defective processing of plastid transcripts. Notably, all *ise2* alleles cause developmental arrest at the torpedo stage of embryogenesis (16), coincident with the time of onset of photosynthesis.

Are mitochondria, like plastids, indispensible for embryogenesis? Mitochondria in mature green tissues have three main functions: (*i*) generation of ATP by oxidative phosphorylation, (*ii*) photorespiration, and (*iii*) supply of carbon backbones for nitrogen assimilation in chloroplasts (53, 54). Photorespiration is unlikely to occur in embryos because of high CO_2 concentrations, and amino acids are supplied to the embryo by the mother plant, negating the need for amino acid metabolism (54). Examination of mitochondrial *emb* genes from the SeedGenes database (Table S3) reveals mutations in mitochondrial translation [*pentatricopeptide repeat* (*PPR*), *tRNA synthase*, and ribosomal genes] or the mETC (e.g., *A. thaliana CYTOCHROME C MATURATION H ortholog*, *A. thaliana SULFUR E*, *A. thaliana FRATAXIN HOMOLOG*). Genes encoding enzymes with critical roles in photorespiration or nitrogen assimilation are not represented in the present mitochondrial *emb* collection, suggesting that these functions are not essential during embryogenesis.

The likely function of the ISE1 DEAD-box RNA helicase is to process mitochondrial transcripts. The *ise1-1* allele used here contains a single point mutation resulting in the G228E mutation in the conserved GG loop. The GG loop is essential for direct binding to RNA (55), and the substitution of a charged residue, glutamic acid, for uncharged glycine in the *ise1-1* mutation likely abolishes its RNA binding activity. The *ise1-3* is a transfer-DNA (T-DNA) insert near the 5′end of the gene, and mutant embryos arrest at the globular stage of development; this phenotype likely represents the null mutant, highlighting that ISE1 is essential, and the importance of mitochondrial function in the early stages of embryogenesis long before photosynthesis begins.

Communication Between Organelles and the Nucleus. Our data underscore the importance of organelle-nuclear communication in the plant cell (Fig. 6). The mitochondrial and plastid genomes encode only a small fraction of the proteins required to perform their essential functions. In *A. thaliana*, the mitochondrial genome encodes only 33 of the estimated more than 1,000 mitochondrial proteins (56); the remaining mitochondrial proteins are nucleus-encoded and posttranslationally imported into mitochondria. Similarly, the chloroplast imports greater than 95% of the 1,000–3,000 chloroplast proteins (22). It is therefore imperative that nuclear gene expression is coordinated with the

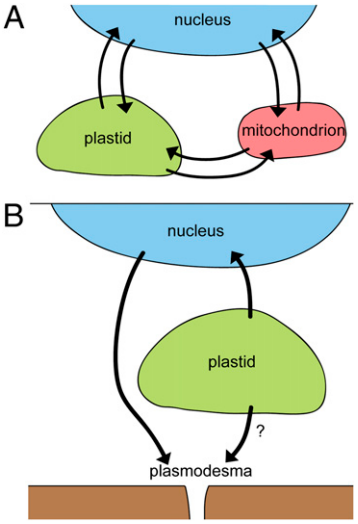

Fig. 6. Model illustrating interorganelle signaling and ONPS. (*A*) Plastids signal to the nucleus, eliciting changes in expression of genes encoding plastid components and also mitochondrial components, a phenomenon called CRR. Mitochondria also signal the nucleus to regulate expression of mitochondrial and plastid-related genes (MRR). Plastids and mitochondria also signal directly with each other. (*B*) ONPS. Chloroplast homeostasis signals the nucleus to regulate the expression of genes for PD structure and function.

metabolic status of mitochondria and plastids. The process of organelle-to-nucleus signaling is broadly referred to as retrograde signaling.

The functions of plastids and mitochondria are intimately linked through metabolism, energy status, and the maintenance and modulation of cellular redox state. Not surprisingly, therefore, mitochondrial retrograde regulation (MRR) and chloroplast retrograde regulation (CRR) share common pathways and intermediates, including signals derived from ROS (57). There also appears to be unique signaling from each organelle to the nucleus. Fig. 6*A* illustrates chloroplast-mitochondria-nucleus cross-talk, wherein signaling between each organelle and the nucleus may lead to altered expression of products targeted to itself or the other organelle.

Genetic screens for mutants defective in CRR pathways led to the identification of six genes, *GENOMES UNCOUPLED* (*GUN*) *1* through *GUN6* (58–60). *GUN2* through *GUN6* participate directly in the plastid tetrapyrrole biosynthetic pathway, and their mutation leads to aberrant accumulation of metabolic intermediates. Hemes, and other tetrapyrroles, are therefore candidate signals for CRR (60, 61). The other GUN protein, GUN1, is a plastid-localized PPR protein (60). PPR proteins belong to a large family (>450 members) of RNA-binding proteins that typically function in RNA processing in plastids and mitochondria (24, 44). In one model, GUN1 promotes the activity of the transcriptional regulator ABSCISIC ACID INSENSITIVE 4 (ABI4) to inhibit the nuclear transcription of *LIGHT HARVESTING COMPLEX B* (*LHCB*) genes (62). ABI4 is a potential master regulator of nuclear gene expression in response to plastid signals (62). A second model for CRR suggests that GUN1 represses the activity of the redundant GOLDEN 2-LIKE (GLK) 1 and GLK2 transcription factors, which would otherwise promote the transcription of *LHCB* genes. GLK transcription factors are implicated in inducing nuclear gene expression in response to plastid signaling (63), and GLK1 and GLK2 have partially redundant functions in regulating chloroplast development (64).

Because *ise1* and *ise2* mutant seeds show decreased transcription of *LHCB* genes, we expected to find altered expression of the *GUN1/ABI4* and *GUN1/GLK* pathways. Indeed, *GLK2* is repressed in *ise1* tissues and *GUN1* is induced in *ise2* mutants (Fig. 4*B* and Dataset S1). Thus, the GUN1/GLK CRR pathway is affected in *ise1* and a GUN1-dependent CRR pathway is also likely operating in *ise2*. Other possible CRR signaling molecules are misexpressed on loss of ISE1 or ISE2: *GUN5* is repressed in both mutants, and *GUN6* is induced in *ise1* (Fig. 4*B*).

Redox in Intercellular Communication. CRR and MRR are both initiated by changes to redox states in the plastids and mitochondria as a result of ROS production (57). Recently, ROS, and presumably redox signaling, has been implicated in regulating intercellular transport. Defective mitochondria in *ise1* mutant embryos or *ISE1*-silenced leaves and treatment with agents that cause anoxia result in ROS accumulation and increased intercellular transport (17, 65). An independent mutant with decreased PD transport, *gfp arrested traffic1* (*gat1*), also produces excess ROS (66). *GAT1* encodes a plastid thioredoxin, implying that increased chloroplast-generated ROS leads to decreased intercellular transport. These data suggest that the site of ROS synthesis is critical in determining PD-mediated intercellular transport. Indeed, chemical treatments to induce oxidative redox shifts in mitochondria or plastids have opposite effects on PD transport. Salicylhydroxamic acid or paraquat induces oxidative shifts in mitochondria or plastids, resulting in increased or decreased PD transport, respectively (67). Further, the redox states of mitochondria and plastids are distinct in tissues lacking ISE1 vs. ISE2. Following *ISE1* silencing, mitochondria are more oxidized and plastids are more reduced, and following *ISE2* silencing, plastids are more reduced (67). These data reiterate that oxidized mitochondria lead to increased PD transport and reveal that reduced plastids increase PD transport.

Why is the site of ROS generation important in modulating different outcomes? Producing ROS in different organelles or organelle compartments can rapidly alter redox states, and hence signaling. Different outcomes are dependent on the specific nature of the downstream signaling transduction pathway coupled to a given ROS sensor in any compartment (68). It is not surprising then that PD are differentially regulated in response to differing ROS levels, and hence redox signals, from plastids vs. mitochondria. Thus, PD are poised to sense the metabolic status of the cell, as modulated by plastid and mitochondrial redox states, facilitating the transport of pertinent molecules and signals among cells to coordinate growth, development, defense, and death.

Conclusions

Our data provide strong evidence linking intracellular communication to intercellular transport. Although CRR and MRR have been previously observed (highlighted in Fig. 6*A*), our data suggest a previously undescribed communication pathway that we dub organelle–nucleus–plasmodesmata signaling (ONPS). ONPS is dependent on the critical interplay between CRR and MRR (Fig. 6). We propose that the chloroplast is the command center for nuclear genes that specifically encode products that alter PD form/function (Fig. 6*B*). This hypothesis is based on the considerable alteration of nuclear genes encoding plastid products in both *ise1* and *ise2*, implying that loss of plastid function leads to increased PD formation/function. Given their central role in carbon metabolism, sensing and responding to various stresses and pathogens, and numerous secondary metabolic processes, disruption of plastid function may provoke the cell to increase communication with its neighbors as a means to obtain or disperse important metabolites and signaling molecules.

Several exciting questions immediately arise. How does ONPS lead to altered PD structure in the cell wall? We identified potential cell wall-modifying genes that may be involved in PD formation and function. Understanding the regulation of such

genes may illuminate how the cell integrates signals to regulate intercellular transport. What are the signals involved in ONPS? Greater insights into the role of ROS in regulating intercellular transport will be necessary for understanding how redox state is used to communicate the physiological state of organelles to the nucleus and then to neighboring cells to coordinate growth, development, and defense.

Materials and Methods

Microscopy. ***Confocal microscopy.*** Leaves of 4-wk-old *N. benthamiana* plants were infiltrated with *Agrobacterium tumefaciens* cultures carrying an *ISE2-GFP* expression cassette (16). Images were collected 48 h later with either a Zeiss LSM 510 with Meta detector or a Zeiss LSM 710 confocal microscope (Carl Zeiss, Inc.).

Transmission EM. Samples for transmission EM were prepared and imaged as described previously (18). Briefly, embryos or leaf discs were frozen at high pressure, freeze-substituted in acetone containing 1% osmium tetroxide plus 0.1% uranyl acetate, and infiltrated with Epon/Araldite Resin (Ted Pella, Inc.). Sections 60 nm thick were stained with methanolic uranyl acetate and lead citrate. Images were collected with a Philips Tecnai 12 TEM (FEI) fitted with an Ultra Scan 1000 CCD camera (Gatan, Inc.).

Virus-Induced Gene Silencing. Virus-induced gene silencing of *ISE1* and *ISE2* was performed as described previously (18). Briefly, two leaves of 3-wk-old *N. benthamiana* plants were infiltrated with *A. tumefaciens* cultures carrying relevant TRV constructs. Plants were kept on light carts under 100 μmol of photons per $m^{-2}{\cdot}s^{-1}$ of light for 24 h a day for 2 wk before observation. Photographs of upper, silenced leaves were taken with a Nikon D60 camera (Nikon, Inc.).

Seed Collection and RNA Sample Preparation. Heterozygous *ise1-1* and *ise2-1* *A. thaliana* plants were grown in long day conditions (16 h light/8 h dark) in a growth chamber at 22 °C under 120 μmol of photons per $m^{-2}{\cdot}s^{-1}$ of light. Siliques containing midtorpedo stage embryos were gently opened with forceps. Mutant seeds were identified by their white color compared with green WT seedlings, and they were collected and placed in liquid nitrogen before being transferred to a freezer at −80 °C for storage. WT sibling embryos also were collected and frozen. Approximately 100 mutant seeds were collected for each of the three genotypes. Duplicate sets of seeds were collected three times from independent groups of plants grown under identical conditions for a total of 18 samples. One set of each pooled sample was used for microarray studies, and the other was used for quantitative PCR analysis.

Fifty microliters of RNA Later (Ambion) was added to each of the three biological replicates in microcentrifuge tubes, and samples were ground with pestles. Total RNA was extracted using a Plant RNeasy Mini Kit (QIAGEN), following the manufacturer's instructions. The extracted RNA was quantified using a 2100 Bioanalyzer (Agilent). Four hundred nanograms of total RNA from each sample was converted to cDNA, amplified to give 4 μg of DNA, and then labeled for hybridization to the arrays using the Applause WT-Amp Plus ST System (NuGen Technologies, Inc.) according to the manufacturer's instructions.

Microarray Hybridization and Data Analysis. *Arabidopsis* GeneChip 1.0R tiling arrays were obtained from Affymetrix, Inc. cDNA hybridization to chips was performed according to Affymetrix protocols, and slides were scanned using a GeneChip Scanner 3000 7G (Affymetrix, Inc.) following the manufacturer's recommendations. Data analysis was performed with the Partek Genomics Suite (Partek Incorporated). Robust multiarray averaging was used for normalization of expression values ($\log_2$) among replicates and for background correction. All necessary quality control steps, including examination of correlations among samples, were taken. Genes with twofold or greater change were identified with one-way ANOVA ($P < 0.05$). Gene functions based on the latest The Arabidopsis Information Resource (TAIR) releases were assigned with MAPMAN (69), VirtualPlant (70), or the TAIR database (www.arabidopsis.org), and they were then assimilated with the most recent literature.

RT Quantitative Real-Time PCR. RNA was extracted from seeds as described for microarray samples. First-strand cDNA synthesis was carried out with Invitrogen SuperScript III Reverse Transcriptase (Life Technologies) according to the manufacturer's instructions. Quantitative PCR was performed with a DyNAmo HS SYBR Green qPCR Kit (Finnzymes Oy.) using the Opticon Real-Time PCR Detection System (Bio-Rad Laboratories, Inc.).

ACKNOWLEDGMENTS. We thank Dr. Julius Lucks for programming assistance and Dr. Marisa Otegui for preparation of embryos for transmission EM. This work was funded by a University of California, Berkley Miller Institute for Basic Research in Science postdoctoral fellowship (to T.M.B.-S.) and National Institutes of Health Grant GM45244 (to P.C.Z.). J.O.B. was funded, in part, by a National Institutes of Health National Research Service Award Trainee appointment on Grant T32 GM 007127 and by National Institutes of Health Grant GM45244 (to P.C.Z.).

1. Ehlers K, Kollmann R (2001) Primary and secondary plasmodesmata: Structure, origin, and functioning. *Protoplasma* 216:1–30.
2. Heinlein M, Epel BL (2004) Macromolecular transport and signaling through plasmodesmata. *Int Rev Cytol* 235:93–164.
3. Burch-Smith TM, Stonebloom S, Xu M, Zambryski PC (2011) Plasmodesmata during development: Re-examination of the importance of primary, secondary, and branched plasmodesmata structure versus function. *Protoplasma* 248:61–74.
4. Faulkner C, Maule A (2011) Opportunities and successes in the search for plasmodesmal proteins. *Protoplasma* 248:27–38.
5. Simpson C, Thomas C, Findlay K, Bayer E, Maule AJ (2009) An Arabidopsis GPI-anchor plasmodesmal neck protein with callose binding activity and potential to regulate cell-to-cell trafficking. *Plant Cell* 21:581–594.
6. Levy A, Erlanger M, Rosenthal M, Epel BL (2007) A plasmodesmata-associated beta-1,3-glucanase in Arabidopsis. *Plant J* 49:669–682.
7. White RG, Badelt K, Overall RL, Vesk M (1994) Actin associated with plasmodesmata. *Protoplasma* 180:169–184.
8. Radford JE, White RG (1998) Localization of a myosin-like protein to plasmodesmata. *Plant J* 14:743–750.
9. Yahalom A, Lando R, Katz A, Epel BL (1998) A calcium-dependent protein kinase is associated with maize mesocotyl plasmodesmata. *J Plant Physiol* 153:354–362.
10. Baluska F, Samaj J, Napier R, Volkmann D (1999) Maize calreticulin localizes preferentially to plasmodesmata in root apex. *Plant J* 19:481–488.
11. Lee JY, et al. (2005) Plasmodesmal-associated protein kinase in tobacco and Arabidopsis recognizes a subset of non-cell-autonomous proteins. *Plant Cell* 17: 2817–2831.
12. Thomas CL, Bayer EM, Ritzenthaler C, Fernandez-Calvino L, Maule AJ (2008) Specific targeting of a plasmodesmal protein affecting cell-to-cell communication. *PLoS Biol* 6:e7.
13. Raffaele S, et al. (2009) Remorin, a solanaceae protein resident in membrane rafts and plasmodesmata, impairs potato virus X movement. *Plant Cell* 21:1541–1555.
14. Fernandez-Calvino L, et al. (2011) Arabidopsis plasmodesmal proteome. *PLoS ONE* 6: e18880.
15. Kim I, Hempel FD, Sha K, Pfluger J, Zambryski PC (2002) Identification of a developmental transition in plasmodesmatal function during embryogenesis in Arabidopsis thaliana. *Development* 129:1261–1272.
16. Kobayashi K, Otegui MS, Krishnakumar S, Mindrinos M, Zambryski P (2007) INCREASED SIZE EXCLUSION LIMIT 2 encodes a putative DEVH box RNA helicase involved in plasmodesmata function during Arabidopsis embryogenesis. *Plant Cell* 19: 1885–1897.
17. Stonebloom S, et al. (2009) Loss of the plant DEAD-box protein ISE1 leads to defective mitochondria and increased cell-to-cell transport via plasmodesmata. *Proc Natl Acad Sci USA* 106:17229–17234.
18. Burch-Smith TM, Zambryski PC (2010) Loss of INCREASED SIZE EXCLUSION LIMIT (ISE)1 or ISE2 increases the formation of secondary plasmodesmata. *Curr Biol* 20:989–993.
19. Emanuelsson O, Brunak S, von Heijne G, Nielsen H (2007) Locating proteins in the cell using TargetP, SignalP and related tools. *Nat Protoc* 2(4):953–971.
20. Ichikawa T, et al. (2006) The FOX hunting system: An alternative gain-of-function gene hunting technique. *Plant J* 48:974–985.
21. Zybailov B, et al. (2008) Sorting signals, N-terminal modifications and abundance of the chloroplast proteome. *PLoS One* 3:e1994.
22. Olinares PD, Ponnala L, van Wijk KJ (2010) Megadalton complexes in the chloroplast stroma of Arabidopsis thaliana characterized by size exclusion chromatography, mass spectrometry, and hierarchical clustering. *Mol Cell Proteomics* 9:1594–1615.
23. Mansfield SG, Briarty LG (1991) Early embryogenesis in *Arabidopsis thaliana*: II. The developing embryo. *Can J Bot* 69:461–476.
24. Jacobs J, Kück U (2011) Function of chloroplast RNA-binding proteins. *Cell Mol Life Sci* 68:735–748.
25. Foyer CH, Noctor G (2005) Redox homeostasis and antioxidant signaling: A metabolic interface between stress perception and physiological responses. *Plant Cell* 17: 1866–1875.
26. Zavaliev R, Ueki S, Epel BL, Citovsky V (2011) Biology of callose (β-1,3-glucan) turnover at plasmodesmata. *Protoplasma* 248:117–130.
27. Laubinger S, et al. (2008) At-TAX: A whole genome tiling array resource for developmental expression analysis and transcript identification in Arabidopsis thaliana. *Genome Biol* 9:R112.
28. Matsui A, et al. (2008) Arabidopsis transcriptome analysis under drought, cold, high-salinity and ABA treatment conditions using a tiling array. *Plant Cell Physiol* 49: 1135–1149.
29. Okamoto M, Seki M (2011) Expression profile and 5′-terminal structure of Arabidopsis antisense transcripts expressed in seeds. *Plant Signal Behav* 6:691–693.

30. Spencer MW, Casson SA, Lindsey K (2007) Transcriptional profiling of the Arabidopsis embryo. *Plant Physiol* 143:924–940.
31. Zavaliev R, Sagi G, Gera A, Epel BL (2010) The constitutive expression of Arabidopsis plasmodesmal-associated class 1 reversibly glycosylated polypeptide impairs plant development and virus spread. *J Exp Bot* 61:131–142.
32. Scheller HV, Ulvskov P (2010) Hemicelluloses. *Annu Rev Plant Biol* 61:263–289.
33. Carpita NC (2011) Update on mechanisms of plant cell wall biosynthesis: How plants make cellulose and other (1->4)-β-D-glycans. *Plant Physiol* 155:171–184.
34. Eklöf JM, Brumer H (2010) The XTH gene family: An update on enzyme structure, function, and phylogeny in xyloglucan remodeling. *Plant Physiol* 153:456–466.
35. Yokoyama R, Nishitani K (2001) A comprehensive expression analysis of all members of a gene family encoding cell-wall enzymes allowed us to predict cis-regulatory regions involved in cell-wall construction in specific organs of Arabidopsis. *Plant Cell Physiol* 42:1025–1033.
36. Becnel J, Natarajan M, Kipp A, Braam J (2006) Developmental expression patterns of Arabidopsis XTH genes reported by transgenes and Genevestigator. *Plant Mol Biol* 61: 451–467.
37. Vissenberg K, et al. (2005) Differential expression of AtXTH17, AtXTH18, AtXTH19 and AtXTH20 genes in Arabidopsis roots. Physiological roles in specification in cell wall construction. *Plant Cell Physiol* 46:192–200.
38. Sampedro J, Cosgrove DJ (2005) The expansin superfamily. *Genome Biol* 6:242.
39. Giraud E, Van Aken O, Ho LH, Whelan J (2009) The transcription factor ABI4 is a regulator of mitochondrial retrograde expression of ALTERNATIVE OXIDASE1a. *Plant Physiol* 150:1286–1296.
40. Binder S, Holzle A, Jonieta C (2011) RNA process and RNA stability in plant mitochondria. *Plant Mitochondria, Advances in Plant Biology*, ed Kempken F (Springer, New York), Vol 1, pp 107–130.
41. Barbrook AC, Howe CJ, Kurniawan DP, Tarr SJ (2010) Organization and expression of organellar genomes. *Philos Trans R Soc Lond B Biol Sci* 365:785–797.
42. Marienfeld J, Unseld M, Brennicke A (1999) The mitochondrial genome of Arabidopsis is composed of both native and immigrant information. *Trends Plant Sci* 4:495–502.
43. Bryant N, Lloyd J, Sweeney C, Myouga F, Meinke D (2011) Identification of nuclear genes encoding chloroplast-localized proteins required for embryo development in Arabidopsis. *Plant Physiol* 155:1678–1689.
44. Stern DB, Goldschmidt-Clermont M, Hanson MR (2010) Chloroplast RNA metabolism. *Annu Rev Plant Biol* 61:125–155.
45. Kollmann R, Glockmann C (1991) Studies on graft unions. III. On the mechanism of secondary formation of plasmodesmata at the graft interface. *Protoplasma* 165: 71–85.
46. Kollmann R, Glockmann C (1999) Multimorphology and nomenclature of plasmodesmata in higher plants. *Plasmodesmata: Structure, Function, Role in Cell Communication*, eds van Bel AJE, van Kesteren WJP (Springer, Heidelberg), pp 149–172.
47. Meinke DW, Sussex IM (1979) Isolation and characterization of six embryo-lethal mutants of Arabidopsis thaliana. *Dev Biol* 72:62–72.
48. Tzafrir I, et al. (2004) Identification of genes required for embryo development in Arabidopsis. *Plant Physiol* 135:1206–1220.
49. Meinke D, Muralla R, Sweeney C, Dickerman A (2008) Identifying essential genes in Arabidopsis thaliana. *Trends Plant Sci* 13(9):483–491.
50. Hsu SC, Belmonte MF, Harada JJ, Inoue K (2010) Indispensable Roles of Plastids in Arabidopsis thaliana Embryogenesis. *Curr Genomics* 11:338–349.
51. Bleichert F, Baserga SJ (2007) The long unwinding road of RNA helicases. *Mol Cell* 27: 339–352.
52. Jankowsky E, Fairman ME (2007) RNA helicases—One fold for many functions. *Curr Opin Struct Biol* 17:316–324.
53. Yoshida K, Noguchi K (2011) Interaction between chloroplasts and mitochondria: Activity, function and regulation of the mitochondrial respiratory system during photosynthesis. *Plant Mitochondria*, ed Kempken F (Springer, New York), pp 383–409.
54. Schwender J, Shachar-Hill Y, Ohlrogge JB (2006) Mitochondrial metabolism in developing embryos of Brassica napus. *J Biol Chem* 281:34040–34047.
55. Sengoku T, Nureki O, Nakamura A, Kobayashi S, Yokoyama S (2006) Structural basis for RNA unwinding by the DEAD-box protein Drosophila Vasa. *Cell* 125:287–300.
56. Giegé P, Sweetlove LJ, Cognat V, Leaver CJ (2005) Coordination of nuclear and mitochondrial genome expression during mitochondrial biogenesis in Arabidopsis. *Plant Cell* 17:1497–1512.
57. Rhoads DM (2011) Plant mitochondrial retrograde regulation. *Plant Mitochondria*, ed Kempken F (Springer, New York), Vol 1, pp 411–437.
58. Susek RE, Ausubel FM, Chory J (1993) Signal transduction mutants of Arabidopsis uncouple nuclear CAB and RBCS gene expression from chloroplast development. *Cell* 74:787–799.
59. Mochizuki N, Brusslan JA, Larkin R, Nagatani A, Chory J (2001) Arabidopsis genomes uncoupled 5 (GUN5) mutant reveals the involvement of Mg-chelatase H subunit in plastid-to-nucleus signal transduction. *Proc Natl Acad Sci USA* 98:2053–2058.
60. Woodson JD, Perez-Ruiz JM, Chory J (2011) Heme synthesis by plastid ferrochelatase I regulates nuclear gene expression in plants. *Curr Biol* 21:897–903.
61. Beale SI (2011) Chloroplast signaling: Retrograde regulation revelations. *Curr Biol* 21: R391–R393.
62. Koussevitzky S, et al. (2007) Signals from chloroplasts converge to regulate nuclear gene expression. *Science* 316:715–719.
63. Kakizaki T, et al. (2009) Coordination of plastid protein import and nuclear gene expression by plastid-to-nucleus retrograde signaling. *Plant Physiol* 151:1339–1353.
64. Fitter DW, Martin DJ, Copley MJ, Scotland RW, Langdale JA (2002) GLK gene pairs regulate chloroplast development in diverse plant species. *Plant J* 31:713–727.
65. Cleland RE, Fujiwara T, Lucas WJ (1994) Plasmodesmal-mediated cell-to-cell transport in wheat roots is modulated by anaerobic stress. *Protoplasma* 178:81–85.
66. Benitez-Alfonso Y, et al. (2009) Control of Arabidopsis meristem development by thioredoxin-dependent regulation of intercellular transport. *Proc Natl Acad Sci USA* 106:3615–3620.
67. Stonebloom S, et al. Redox states of plastids and mitochondria differentially regulate intercellular transport via plasmodemata. *Plant Physiol*, in press.
68. Foyer CH, Noctor G (2003) Redox sensing and signalling associated with reactive oxygen in chloroplasts, peroxisomes and mitochondria. *Physiol Plant* 119:355–364.
69. Thimm O, et al. (2004) MAPMAN: A user-driven tool to display genomics data sets onto diagrams of metabolic pathways and other biological processes. *Plant J* 37: 914–939.
70. Katari MS, et al. (2010) VirtualPlant: A software platform to support systems biology research. *Plant Physiol* 152:500–515.